Atmos. Chem. Phys. Discuss., 11, 5043–5078, 2011
www.atmos-chem-phys-discuss.net/11/5043/2011/
doi:10.5194/acpd-11-5043-2011
© Author(s) 2011. CC Attribution 3.0 License.

Atmospheric Chemistry and Physics Discussions

This discussion paper is/has been under review for the journal Atmospheric Chemistry and Physics (ACP). Please refer to the corresponding final paper in ACP if available.

Urban organic aerosols measured by single particle mass spectrometry in the megacity of London

M. Dall'Osto[1,*] **and R. M. Harrison**[1]

[1]National Centre for Atmospheric Science, Division of Environmental Health & Risk Management, School of Geography, Earth & Environmental Sciences University of Birmingham Edgbaston, Birmingham B15 2TT, UK
[*]now at: Institute of Environmental Assessment and Water Research (IDÆA) Consejo Superior de Investigaciones Científicas (CSIC) C/LLuis Solé i Sabarís S/N 08028 Barcelona, Spain

Received: 6 January 2011 – Accepted: 25 January 2011 – Published: 10 February 2011

Correspondence to: R. M. Harrison (r.m.harrison@bham.ac.uk)

Published by Copernicus Publications on behalf of the European Geosciences Union.

Abstract

During the month of October 2006, as part of the REPARTEE-I experiment (Regent's Park and Tower Environmental Experiment) an Aerosol Time-Of-Flight Mass Spectrometer (ATOFMS) was deployed at an urban background location in the city of London, UK. Fifteen particle types were classified, some of which were accompanied by Aerosol Mass Spectrometer (AMS) quantitative aerosol mass loading measurements (Dall'Osto et al., 2009a, b). In this manuscript the origins and properties of four particle types associated with locally generated aerosols, independent of the air mass type advected into London, are examined. One particle type, originating from lubricating oil (referred to as Ca-EC), was associated with morning rush hour traffic emissions. A second particle type, composed of both inorganic and organic species (called Na-EC-OC), was found enhanced in particle number concentration during evening time periods, and is likely to originate from a source operating at this time of day, or more probably from condensation of semi-volatile species, and contains both primary and secondary components. A third class, internally mixed with organic carbon and sulphate (called OC), was found to spike both in the morning and evenings. The fourth class (SOA-PAH) exhibited maximum frequency during the warmest part of the day, and a number of factors point towards secondary production from traffic-related volatile aromatic compounds. Single particle mass spectra of this particle type showed an oxidized polycyclic aromatic compound signature. Finally, a comparison of ATOFMS particle class data is made with factors obtained by Positive Matrix Factorization from AMS data.. Both the Ca-EC and OC particle types correlate with the AMS HOA primary organic fraction (R^2 = 0.65 and 0.50 respectively), and Na-EC-OC, but not SOA-PAH, which correlates weakly with the AMS OOA secondary organic aerosol factor (R^2 = 0.35). A detailed analysis was conducted to identify ATOFMS particle type(s) representative of the AMS COA cooking aerosol factor, but no convincing associations were found.

1 Introduction

Tropospheric particles contain a significant and variable fraction of organic material, ranging from 20% to 90% of the fine particulate mass (Kanakidou et al., 2005) and divide into two broad categories termed primary and secondary. Primary particles are directly emitted from combustion sources, including heavy and light duty vehicles, wood smoke, cooking activities, industries and many others. Once primary particles are emitted they are modified in the presence of various atmospheric oxidants, yielding secondary particles with distinctly different chemical and physical properties compared to their precursor primary particles (Donahue et al., 2009). Secondary organic aerosol (SOA) is also formed from reactions of VOC. SOA consists of a mixture of oxygenated organic species dependent on the degree of processing of the aerosol in the atmosphere, and the precise mechanisms of formation and evolution of SOA are still highly uncertain. Models informed by chamber experiments do not always capture the variability of observed SOA loadings, and often predict far less SOA than is observed. This underestimation of SOA strongly suggests the importance of additional pathways of SOA formation not typically studied in laboratory experiments or included in models. The chemistry of the formation and continuing transformation of low-volatility species in the atmosphere has been the subject of recent review articles (Kanakidou et al., 2005; Goldstein and Galbally, 2007; Kroll and Seinfeld, 2008). In particular, Kroll and Seinfeld (2008) reviewed the three primary factors that determine the SOA-forming potential of organic compounds in the atmosphere: (1) oxidation reactions of gas-phase organic species; (2) reactions in the particle (condensed) phase and (3) the extent to which these reactions occur as a result of ongoing chemistry.

Until recently, organic particulate material was simply classified as either primary or secondary with the primary component being treated in models as nonvolatile and inert. However, the simplified models failed to explain a number of key aspect of the aerosols, including the highly oxygenated nature of ambient OA and the high concentrations of OA during periods of high photochemical activity. Recent studies have

shown that semi-volatile components of primary aerosols desorb into the gas phase during aerosol transport, thereby undergoing oxidation in the gas phase, leading to SOA formation (Robinson et al., 2007). This opens the possibility that low-volatility gas-phase precursors, including long chain n-alkanes, PAHs and large olefins, are a potentially large source of SOA.

Polycyclic Aromatic Hydrocarbons (PAH) have been identified as a major component in emissions from diesel engines and wood burning sources (Schauer et al., 1999, 2001). The photo-oxidation of these compounds has been shown to yield high molecular weight (MW) oxygenated compounds (Sasaki et al., 1997; Bunce et al., 1997; Wang et al., 2007), which can partition into the particle phase and lead to significant SOA formation (Mihele et al., 2002). Current atmospheric models do not normally include secondary organic aerosol (SOA) production from gas-phase reactions of polycyclic aromatic hydrocarbons (PAHs). Chan et al. (2009) reported a laboratory study of secondary organic aerosol formation from photooxidation of naphthalene and alkylnaphthalenes. Although the gas-phase emissions were dominated by low molecular weight aromatics, these compounds were estimated to account for only 14% of the SOA formed in the first 3 h of photooxidation. The estimate is consistent with laboratory results of photooxidation of diesel exhaust (Robinson et al., 2007), in which the "known" consisting primarily of single-ring aromatics gas phase precursors, account for at most 15% of the SOA formed. On the contrary, although PAH emissions are a factor of 4 lower than those of light aromatics, their relatively fast reaction with OH radicals and high SOA yields lead to significant SOA production in the first 3 h, accounting for 4 times the amount formed from light aromatics. The contribution of PAH to SOA is still significant after 12 h of oxidation, at which point the SOA from PAH is about twice that from light aromatics (Chan et al., 2009).

Whilst biogenic precursors (predominantly monoterpenes) have traditionally been thought to dominate regional SOA formation, anthropogenic compounds may contribute an appreciable fraction of SOA in urban areas. Mono-aromatic hydrocarbons are one of the most abundant types of organic compound found in the urban atmosphere.

Langford et al. (2010) recently reported fluxes and concentrations of volatile organic compounds above central London, estimating that traffic activity was responsible for about 70% of the aromatic compound fluxes. The ultimate photo-oxidation products of many relatively simple mono-aromatic species remain unknown, due to the complexity and low concentrations formed. The incorporation of a mono-aromatic compound into polymeric compounds with acetal polymers was also suggested (Kalberer et al., 2004).

In recent years aerosol mass spectrometry has become available as a powerful tool for the on-line chemical characterization of individual aerosol particles (Murphy, 2007) or small aerosol ensembles (Canagaratna et al., 2007). During the month of October 2006, the REPARTEE-I campaign (Regent's Park and Tower Environmental Experiment) studied atmospheric chemical processes, and particularly those affecting atmospheric aerosol, in London. Two different particle mass spectrometers were deployed: an Aerodyne High-Resolution Time-of-Flight Aerosol Mass Spectrometer (C-ToF-AMS) (Drewnick et al., 2005) and an Aerosol Time-of-Flight Mass Spectrometer (ATOFMS) (Gard et al., 1997). The ATOFMS provides single particle information on the abundance of different types of aerosol particles as a function of particle size with high time resolution, whereas the AMS measures quantitatively precise mass concentrations of the non-refractory aerosol components as well as species-resolved size distributions.

These types of on-line aerosol analysis instrumentation have greatly advanced our understanding of atmospheric chemistry and climate (Sullivan and Prather, 2005). Whilst the AMS has provided advances in the source apportionment of primary versus secondary organic aerosol components (Canagaratna et al., 2007), the ATOFMS has less adequate source apportionment capabilities due to the difficulties in quantification of its outputs.

During the REPARTEE-I field study for example, the ATOFMS focused on atmospheric chemical processes (Dall'Osto et al. 2009a, b) whilst a detailed source apportionment analysis of the organic aerosols measured by the AMS is described in Allan et al. (2010). In summary, three contributions were identified in REPARTEE I: secondary Oxygenated Organic Aerosols (OOA, 53%), primary Hydrocarbon-like Organic Aerosol

(HOA, 25%) and primary Cooking Organic Aerosol (COA, 22%). By complementary AMS and ATOFMS analysis, a number of chemical processes could be followed in real time during the REPARTEE experiment. Dall'Osto et al. (2009a) found two types of nitrate-containing aerosols: the first (33.6% of particles by number) appeared to be locally produced in urban locations during nighttime, whilst the second (22.8% of particles by number) was regionally transported from continental Europe. Dall'Osto et al. (2009b) reported on aerosol formation processes during a fog event within the campaign period. An overview of the ATOFMS findings provided by the REPARTEE I campaign can also be found in Harrison et al. (2010). The present study aims to present a detailed analysis of ATOFMS particle classes not described by Dall'Osto et al. (2009a, b). The particle types herein described were predominantly organic particle types presenting systematic diurnal trends persisting over three weeks and therefore attributable to local primary and secondary processes occurring daily at the local scale and independent of whichever air mass type the city of London was exposed to. Aspects of the data are compared with the source attribution results for organic carbon derived from PMF analysis of AMS data collected during the same campaign by Allan et al. (2010).

2 Experimental

2.1 Aerosol sampling

Sampling took place in Regents Park, one of the Royal Parks of London between 4 and 23 October 2006. Regents Park is located in the northern part of central London. The park has an outer ring road called the Outer Circle (4.3 km) and an inner ring road called the Inner Circle. Apart from two link roads between these two, the park is reserved for pedestrians and the ca. 2 km^2 park is mainly open parkland. The sampling site chosen was inside the inner circle, in an open area usually reserved for parking and gardening purposes. All the instruments were housed in a mobile laboratory. The

site was operated as part of the REPARTEE-I experiment (Regent's Park and Tower Environmental Experiment) aiming to study atmospheric chemical processes, and particularly those affecting atmospheric aerosol, in London. Meteorological, gas-phase and aerosol measurements were conducted from the top of a 10 m high tower constructed on site. To minimise sampling losses, aerosol was drawn down a specially designed sampling stack from which it was iso-kinetically sub-sampled into a 2 cm diameter stainless steel tube leading to the mobile laboratory (Harrison et al., 2010). Local meteorological conditions were measured by humidity and temperature probes, and a sonic anemometer which measured the 3-D wind field at the sampling site.

2.2 Instrumentation

The ATOFMS collects bipolar mass spectra of individual aerosol particles. Ambient aerosol is focused into a narrow particle beam for sizes between 100 nm and 3 µm. Using a 2-laser velocimeter particle sizes are determined from particle velocity after acceleration into the vacuum. In addition, the light scattered by the particles is used to trigger a pulsed high power desorption and ionization laser ($\lambda = 266$ nm, about 1 mJ/pulse) which evaporates and ionizes the particle in the centre of the ion source of a bipolar reflectron ToF-MS. Thus, a positive and negative ion spectrum of a single particle are obtained. The mass spectrum is qualitative in that the intensities of the mass spectral peaks are not directly proportional to the component mass but are dependent on the particle matrix, the coupling between the laser and the particle and the shot to shot variability of the laser. However, the ATOFMS can provide quantitative information on particle number as a function of composition; providing a measure of all particle components and can be used to assess mixing state. The ATOFMS provides information on the abundance of different types of aerosol particles as a function of particle size with high time resolution (Gard et al., 1997).

ATOFMS laser desorption/ionization of chemical species in the particles is accomplished using a Nd:YAG laser operating at 266 nm, and PAHs and their heterocyclic analogues present very high molar absorptivity at this wavelength therefore it

is expected that these compounds will be detected among the most easily of all compounds using ATOFMS. The laser fluence of the LDI laser of the ATOFMS was kept very low (0.8–0.9 mJ per pulse) in comparison to other studies (1.3–1.6 mJ). The fragmentation of organic compounds was therefore much reduced (the ionization potential of most PAHs is relatively low), enhancing the detection of high molecular weight species as molecular ions (Silva and Prather, 2000).

In addition to the aerosol mass spectrometers a variety of on-line aerosol instruments were deployed to measure different physical characteristics of the ambient aerosol. A Multi-Angle Absorption Photometer (MAAP, Thermo Electron) (Petzold and Schonlinner, 2004) was used to measure 1-min averages of the ambient black carbon concentrations. Moreover, Dichotomous Partisol-Plus Model 2025 sequential air samplers, fitted with PM10 inlets were deployed for collecting fine ($PM_{2.5}$) and coarse ($PM_{2.5-10}$) fractions. A number of other instruments were used during the REPARTEE-I campaign but are not listed here since their data are not discussed in this paper. Local meteorology was determined by a Weather Transmitter WXT510 (Vaisala Ltd, Birmingham) probe. Gas measurements were obtained by Thermo Environment 42CTL chemiluminescence gas analyser with thermal converter and by Thermo Environment 49C photometric UV analyzer for NO_x and ozone, respectively.

2.3 Data analysis

The ATOFMS was deployed at Regents Park for 19 days, between 4 October 2006 at 17:00 and 22 October 2006 at 23:00. In total, 153 595 particles were hit by the ATOFMS. The TSI ATOFMS dataset was imported into YAADA (Yet Another ATOFMS Data Analyzer) and single particle mass spectra were grouped with Adaptive Resonance Theory neural network, ART-2a (Song et al., 1999). The parameters used for ART-2a in this experiment were: learning rate 0.05, vigilance factor 0.85, and iterations 20. Further details of the parameters can be found elsewhere (Dall'Osto and Harrison, 2006). An ART-2a area matrix (AM) of a particle cluster represents the average intensity for each *m/z* value for all particles within a group. An ART-2a AM therefore

reflects the typical mass spectrum of the particles within a group. The ART-2a algorithm generated 306 clusters used to describe the dataset. By manually merging similar clusters (Dall'Osto and Harrison, 2006), the total number of clusters describing the whole database was reduced to 15. It is important to stress the fact that whilst the ATOFMS provides important information on the mixing state of the aerosols and temporal trends of unique particle types over time, the total number of particles sampled by the instrument does not have quantitative meaning without extensive calibrations as it is biased by a number of sampling artifacts (Dall'Osto et al., 2006). Whilst some semi-quantitative ATOFMS measurements have been reported (i.e. Qin et al., 2006) in the literature, no attempt was herein tried to scale ATOFMS measurements with other techniques.

3 Results

Twelve of the 15 clusters contained mass spectral peaks characteristic of organic containing aerosols, accounting for 83.7% of the total particles classified (see Table 1). Of these, the 3 main clusters were associated also with nitrate aerosol and are already discussed in Dall'Osto et al. (2009a). Two specific ATOFMS clusters associated with secondary organic aerosol production during a fog event have already been discussed in Dall'Osto et al. (2009b). This paper focuses on four particle types named Ca-EC (Calcium – Elemental Carbon), OC (Organic Carbon), Na-EC-OC (Sodium – Elemental Carbon – Organic Carbon) and SOA-PAH (Secondary Organic Aerosols – Polycyclic Aromatic Hydrocarbons) accounting for 4.3%, 3.6%, 1.7% and 2.2% (respectively) of the ATOFMS particles classified during the REPARTEE I experiment.

The weather during the field study was characterized by unusually warm conditions for the month of October in the UK (average temperature 14.1 ± 2.8 °C, relative humidity 82.6 ± 10.7%; mean ±1 s.d. of hourly data). The predominant origin of air masses arriving at the receptor was westerly, with Atlantic air masses not strongly influenced by anthropogenic pollution. However, during two periods, air masses arriving at our site

from mainland Europe (mainly France and Poland) were detected on 10–11 October 2006 and on 14–20 October 2006. Local wind direction roses were calculated for all 15 ATOFMS clusters, and ATOFMS particle types associated with regional and continental aerosols were found to be associated predominantly with an easterly origin. ATOFMS particle types characterized by daily diurnal profiles were mainly associated with south and east directions, where main roads bordering the Regents Park are located.

3.1 ATOFMS characterization

3.1.1 ATOFMS mass spectra

The positive and negative ART-2a AMs for the four particle types described are presented in Fig. 1. The mass spectra of cluster Ca-EC (Fig. 1a) show a strong signature due to calcium (*m/z* 40, 56, 57 and 96), EC (*m/z* −36, −48, −60) and OC (*m/z* 27, 29, 43). Strong signals in the negative mass spectrum are associated with nitrate (*m/z* −46, −62), whereas sulphate (*m/z* −97) is almost absent. This is consistent with a source in vehicle exhaust, which is rich in NO_x but depleted in SO_2 due to use of low sulphur fuel. This particle type has previously been associated with combusted lubricating oil emitted by traffic (Spencer et al., 2006; Dall'Osto et al., 2009b).

Figure 1b shows the ART-2a AMs for cluster OC: strong signals due to organic fragments are seen at *m/z* 27, 29, 43, 51, 57 and 63. This particle, by contrast with the Ca-EC type, is internally mixed with both nitrate and sulphate, with a higher signal for the latter. Cluster Na-EC-OC (Fig. 1c) shows a signal at *m/z* 23 for the inorganic component sodium, not seen in other mass spectra presented in Fig. 1 and suggesting a different source. Moreover, beside the OC and EC component associated with the Na-EC-OC particle type, the negative spectra of this particle type also show signals due to inorganic nitrogen (*m/z* −26 [CN] and *m/z* −42 [CNO]), also not seen clearly in the other particle types.

Cluster SOA-PAH presents a unique positive mass spectrum (Figure 1d), with strong peaks at *m/z* 27 $[C_2H_3]^+$ and *m/z* 43 $[(CH_3)CO]^+$. *m/z* 51 $[C_4H_3]^+$, 63 $[C_5H_3]^+$, 77 $[C_6H_5]^+$ and 91 $[C_7H_7]^+$ are indicative of a strong aromatic signature (McLafferty, 1993). In the positive mass spectrum, the major peaks at *m/z* above 100 amu show a series at *m/z* 115, 128, 141, 152, 165, 178, 189, 202, 215, 226, 239 and 252 which is usually attributed to PAH compounds (Gross et al., 2000; Silva and Prather, 2000). Figure 2 shows positive and negative mass spectra of a single particle (aerodynamic diameter 400 nm) belonging to the ATOFMS particle type SOA-PAH. Additional peaks at *m/z* 180, 194, 208, 222, 236, 262 and 276, characteristic of oligomeric species with saturated carbon skeletons separated by Δ14 are present in addition to the PAH series separated by Δ13. Other peaks at *m/z* above 100 can be clearly seen with a series at *m/z* 105, 119, 133 and 147, possibly associated with benzoyl groups and unsaturated or cyclic phenoxy moieties (McLafferty, 1993). The peaks at *m/z* 69, 81 and 95 (particularly the strong peak at *m/z* 95) may represent the exo-sulphur aromatic series (sulphur attached to an aromatic ring) (McLafferty, 1993).

The single particle ATOFMS negative mass spectrum of cluster SOA-PAH (Fig. 2) is dominated by *m/z* −25 and *m/z* −26 (likely to be $[C_2H]^-$ and $[C_2H_2]^-$ respectively) and *m/z* at −49 and *m/z* −73, which are often associated with fragmentation of PAH and unsaturated organic compounds (Silva and Prather, 2000; Spencer et al., 2006). The presence of strongly acidic compounds is indicated by peaks in the negative spectra. Along with the common peak at *m/z* −97 $[HSO_4]^-$, peaks at *m/z* −80 $[SO_3]^-$, *m/z* −81 $[HSO_3]^-$ and *m/z* −64 $[SO_2]^-$ can be seen. The peak at *m/z* −81 suggests the particle is highly acidic (Whiteaker and Prather, 2003). It is interesting to note the almost complete absence of common peaks due to nitrate (i.e. *m/z* −46 $[NO_2]^-$, *m/z* −62 $[NO_3]^-$ and *m/z* −125 $[H(NO_3)_2]^-$. Perhaps the most interesting feature of the negative mass spectrum of Fig. 2 is the presence of other oxygenated aromatic rings indicated by peaks not reported before in ATOFMS mass spectral characterization seen at *m/z* −107, *m/z* −121 and *m/z* −137, characteristic of fragmentation patterns often associated with flavonoids (Cuyckens and Claeys, 2004; Maul et al., 2008). By querying

the whole ATOFMS dataset (about 150 000 single particle mass spectra), it was found that *m/z* −107, *m/z* −121 and *m/z* −137 were unique to this particle type. In summary, the positive and negative ATOFMS mass spectra of particle type SOA-PAH indicate a highly oxidised organic aerosol component internally mixed with acid sulphate species, along with a complex signature at higher *m/z* which is attributable to high molecular weight polyaromatic compounds.

3.1.2 ATOFMS size distributions

ATOFMS size distributions were obtained by scaling the ATOFMS particle number counts with simultaneously collected DMPS and APS particle number size distributions to calibrate inlet efficiencies (Qin et al., 2006). It should be stressed that the size distributions presented in this work have only semi-quantitative meaning, as the ATOFMS efficiency is different for different particles and each broad type of particles exhibits a different hit rate (Dall'Osto et al., 2006, Reinard et al., 2007). Whilst the ATOFMS measures precisely the vacuum aerodynamic diameter of individual particles (0.01 µm resolution), particles were summed between 200 nm and 3500 nm at 100 nm intervals for simplification. Figure 3 shows the size distributions for the four ATOFMS particle types Ca-EC, OC, Na-EC-OC and SOA-PAH. Clusters Ca-EC and OC show a uni-modal distributions peaking in the smallest detectable ATOFMS particle diameter at about 200 nm. The mass spectra of these two particle types described in Sect. 3.1.1, along with the size distributions herein presented, are indicative of a primary origin of these particles. Cluster Na-EC-OC also shows a mode peaking at the smallest sizes, but much less pronounced relative to clusters Ca-EC and OC. Moreover, a second smaller mode can be seen for particle type Na-EC-OC in the coarser region. By contrast to the first three clusters presented so far, cluster SOA-PAH shows a mode peaking at about 350 nm and not peaking at the smallest detectable ATOFMS particle diameter. The coarser mode of cluster SOA-PAH relative to clusters Ca-EC and OC suggests a different origin not related to primary emissions.

3.2 Time trend analysis

3.2.1 Overview of the temporal trends

The temporal trends (3 h resolution) of the four ATOFMS clusters are presented in Fig. 4. Clusters Ca-EC and OC (Fig. 4a) showed maximum abundance during the morning of 13 October 2006, when low wind speed was associated with stagnant conditions, also reflected in high concentrations of primary traffic related species (BC, NO, NO_x, Fig. 4b). Figure 4c shows the temporal profiles of the 3 PMF factor components of the AMS organic matrices described in Allan et al. (2010). The OOA component dominated the periods of 9–10 and 14–20 October 2006 affected by continentally influenced air masses, in which the ATOFMS showed nitrate internally mixed with elemental carbon and organic carbon (Dall'Osto et al., 2009a). Cluster HOA shows its maximum on the morning of 13 October, and other high concentrations during the morning rush hours of 11, 12, 16 and 17 October, correlating with the maximum values of ATOFMS cluster Ca-EC related to primary traffic emissions (Fig. 4a–c). The highest concentrations of cluster SOA-PAH (Fig. 4a) occurred on 11 and 17–20 October, which are also the days where AMS cluster COA presents its higher mass loading concentrations during daytime (Fig. 4c).

3.2.2 Diurnal profiles

The temporal trends derived from a number of other instruments appear in Fig. 5, showing the average diurnal profiles of (a) ATOFMS clusters described in Figure 1, (b) AMS PMF factors as reported in Allan et al. (2010); (c) ozone, NO_x and BC concentrations; (d) relative humidity and temperature and (e) ATOFMS hit particles with *m/z* 55 (peak height > 100). ATOFMS Cluster Ca-EC, as expected from its mass spectra and size distribution, exhibits a maximum during morning rush hours (05:00–09:00) due to primary traffic emissions (Fig. 5a). It correlates strongly with NO_x and BC (Fig. 5c), along with the primary organic aerosol traffic related HOA (Fig. 5b) derived by the AMS (Allan

et al., 2010). During rush hours BC concentrations were around 4 µg m^{-3}, NO_x concentrations about 20 ppb, and HOA about 1.5 µg m^{-3}. A second peak at about 16:00 due to the second traffic rush hour period is evident in Fig. 5 from the ATOFMS cluster Ca-EC and NO_x diurnal trends. Cluster OC (Fig. 5a) also showed a spike in the morning traffic rush hour, reflected by a good correlation with cluster Ca-EC ($R^2 = 0.7$). However, cluster OC also exhibited a second sharper peak during evening hours spiking at about 21:00. Cluster Na-EC-OC did not show as strong a diurnal profile as the previous classes described (Fig. 5a) but a two fold increase occurred between 18:00 and 24:00 relative to the other hours of the day suggesting an additional evening aerosol source or atmospheric process responsible for this particle type. Figure 5a shows that in contrast to the other three ATOFMS particles types presented so far, ATOFMS particle type SOA-PAH exhibits a peak in the middle of the day. This cluster exhibits a bimodal daily trend: the earlier mode starts at about 08:00, as temperature also rises (Fig. 5d) and lasts for about 3 hours. The second mode, peaking at 12:00 and 13:00 is in the hottest part of the day. Concentrations decrease substantially after 14:00, disappearing by about 19:00 (Fig. 5a).

The diurnal profile of particles detected by the ATOFMS containing a peak with significant signal (peak height > 100) at *m/z* 55 (Fig. 5d) is also shown but it is discussed in Sect. 4.

3.2.3 Weekday-weekend trend

An analysis of the weekday-weekend (WD-WE) variation was performed on all 15 clusters derived from the ca. 150 000 single particles detected during the REPARTEE-I campaign. The two clusters with the highest weekday to weekend ratio were found to be cluster Ca-EC (weekdays: 16 ± 15; weekend: 8 ± 6; average ATOFMS counts/hour) and cluster SOA-PAH (15 ± 25; 3 ± 7). Cluster OC was only moderately elevated during weekdays (12 ± 17) over weekends (9 ± 7) whilst no WD-WE oscillation was detected for cluster Na-EC-OC (4 ± 3, 4 ± 5). A WD-WE analysis of other measurements

was also performed in order to compare them with the variation of the ATOFMS clusters. An analysis of the particulate mass loading available for 3 different sites within London during the REPARTEE I campaign (park site "Regents Park" – RP, road site "Marylebone Road" – MR – and 160 m tower "BT tower" – BT –, see Harrison et al., 2010) was carried out, but 16 October 2006 was removed as it exceeded 50 $\mu g\,m^{-3}$ largely due to regional pollutant transport and was not comparable with the other days of the month of October 2006. $PM_{2.5}$ at the Marylebone Road site air monitoring site showed a strong WD-WE variation (26 ± 7, 20 ± 7; $\mu g\,m^{-3}$), whereas the background sites of RP (10 ± 6, 10 ± 7) and BT (10 ± 8, 10.5 ± 9) showed similar values for weekdays and weekend. However, whilst $PM_{2.5}$ at RP did not show a WD-WE variation, traffic markers showed a strong gradient between WD and WE periods, including BC (3.2 ± 1.7, 1.8 ± 0.9; $\mu g\,m^{-3}$), NO (36 ± 52, 9 ± 14) and NO_x (70 ± 54, 35 ± 22). A brief analysis of the primary organic aerosol components described in detail in Allan et al. (2010) showed the traffic HOA component to present a strong WD-WE difference: $1.3 \pm 0.8\,\mu g\,m^{-3}$ and $0.6 \pm 0.5\,\mu g\,m^{-3}$ (respectively) reflecting the BC and NO_x difference of about a factor of two higher during weekdays. Factor COA did not show a strong variation, again only slightly higher during weekdays than weekends: $1.4 \pm 1.1\,\mu g\,m^{-3}$ and $1.2 \pm 0.9\,\mu g\,m^{-3}$, respectively. However, given the fact that AMS factor COA presents two peaks at about 12:00 and 20:00, further separation was required. Factor COA was divided into WD-WE periods, further split between day time (09:00–18:00) and evening time (18:00–24:00). COA-day was found to be about 25% higher during weekdays ($1.03 \pm 0.78\,\mu g\,m^{-3}$) relative to weekend ($0.76 \pm 0.41\,\mu g\,m^{-3}$), whilst a weaker opposite trend was found for evening times (WD: $2.0 \pm 1.3\,\mu g\,m^{-3}$; WE: $2.17 \pm 1.1\,\mu g\,m^{-3}$). HOA presented overall lower values over weekend periods at both day and evening periods, with the former reduced more (about 60%) than the latter (about 20%).

4 Discussion

4.1 Source attribution

The Cluster Ca-EC has previously been associated with primary traffic-related combustion particles in both laboratory (Spencer et al., 2006) and field measurements (Dall'Osto et al., 2009b; Toner et al., 2008) and this study confirms its primary origin from vehicular emissions. Cluster OC presents features pointing towards a primary organic source, similar to cluster Ca-EC; it shows a strong organic carbon signature, a small aerodynamic diameter and peaks in the morning rush hour. However, the cluster OC was internally mixed with sulphate and was elevated also in the evening time. This suggests an additional source occurring in the evening, unlike the cluster Ca-EC which decreases during the evening. The morning peak probably arises from condensation of semi-volatile organic compounds onto sulphate-rich particles, and the evening peak may be due to condensation caused by reductions in air temperature. Cluster Na-EC-OC showed a broader size distribution with a greater proportion of coarser particles and a mass spectrum internally mixed with inorganic species including sodium and nitrogen, peaking during evening hours. Whilst this particle type contains the strongest peak at *m/z* 39, we exclude a biomass origin for a number of reasons. The peak at *m/z* 39 is not only associated with potassium ($[K]^+$ – to which the ATOFMS is especially sensitive), but may also be due to an organic fragment $[C_3H_3]^+$ (Silva and Prather, 2000). The complete absence of common peaks associated with the presence of potassium (i.e. *m/z* 113 $[K_2Cl]^+$ or *m/z* 213 $[K_3SO_4]^+$) and a ratio between *m/z* 39 and *m/z* 41 of about 18 (the isotopic ratio $^{39}K/^{41}K$ is 13.28) strongly suggest that the *m/z* 39 peak is not due to potassium alone, whereas it dominates in biomass combustion particle types, along with other potassium clusters (Silva et al., 1999). This particle type could originate from a number of sources occurring during the evening times but may also arise from physical processes occurring in the atmosphere during evening time when air temperature falls. During the summer of 2003, an ATOFMS was

deployed in another European capital (Dall'Osto and Harrison, 2006) and most of the carbon-containing particles appeared to be a secondary product of atmospheric chemistry and one specific class peaked every night at 22:00, when lower temperature and increased RH values favoured condensation. The secondary particles showed clear internal mixing of organic and inorganic constituents in contrast to their common theoretical treatment as external mixtures. The cluster Na-EC-OC from this London field study shows similar mass spectral features, but does not show the expected diurnal variation.

The cluster SOA-PAH exhibits a unique set of properties, including weekday-weekend variation, maximum frequency during the warmest part of the day, and a mass spectral signature associated with PAH and oxygenated high molecular mass compounds. The fact that cluster SOA-PAH is detected predominantly during weekdays and presents a maximum during the midday hours suggests a photochemical mechanism linked with volatile organic compounds (VOC) arising from traffic activity. The weekday-weekend trend excludes a biogenic source. The mass spectrum of cluster type SOA-PAH was compared with the ATOFMS particle mass spectral libraries. Source signatures, or mass spectral "fingerprints", were obtained by using ATOFMS data from a variety of sources (Toner, 2008). Cluster SOA-PAH did not match exactly any of the 20 different ART2a clusters representative of different cooking related sources, nor any oil, gasoline or diesel combustion source. Finally, it is important to note the absence of any peak associated with common metals (i.e. Ca, Na, K, V) detected in ATOFMS mass spectra of particles originating from primary anthropogenic aerosol sources. The temporal trend of the cluster SOA-PAH suggests that this particle type is short-lived, perhaps due to chemical decomposition. The ATOFMS mass spectrum shows signals usually associated with PAH components already described in Sect. 3.1.1, which point to a primary aerosol source. However, the PAH signature may be related to secondary components, possibly oxidation products of PAHs. Reactions of degradation products may also lead to further secondary compounds. Webb et al. (2006) for example showed the organic aerosol product formed from the

photo-oxidation of o-tolualdehyde contained a diverse range of chemical functionalities including mono-aromatic, carboxylic and carbonyl groups which were inferred to be photochemical by-products but around 3% of the organic content resolved was polycyclic aromatic (PAH) in nature. The ATOFMS is very sensitive to polycyclic aromatic structures, so whilst PAH may be a minor component of the mass of the particle, they can generate a disproportionate fraction of the mass spectral signature. The cluster SOA-PAH does not behave as a typical semi-volatile species whose concentration increases as temperature decreases. The fact that its temporal trend does not correlate with any commonly identified primary aerosol components or markers (Ca-EC from ATOFMS, BC, NO_x, SO_2) excludes a primary aerosol source, and the maximum intensity at noon points towards a photochemical origin. Whilst PAHs are emitted directly from combustion processes, the sources of oxygenated PAH emissions in the atmosphere can be both by direct emission and by tropospheric conversion of PAHs, but quantitative data on the importance of secondary versus primary origins are scarce (Walgraeve et al., 2010). Ning et al. (2007) reported the daily variation in chemical characteristics of urban secondary ultrafine aerosols, showing that afternoon concentrations of oxygenated organic acids and sulfate rose relative to primary organic compounds in the morning and demonstrating that secondary photochemical reactions are a major formation mechanism of ultrafine aerosols in the afternoon. Specifically, the larger decrease in the concentration of non-oxidized PAHs and alkanes compared to CO in the afternoon indicated their possible volatilization and photo-oxidation in addition to dilution. Verma et al. (2009) suggested in a subsequent study that the photochemical transformation of primary emissions during atmospheric aging enhances the toxicological potency of primary particles in terms of generating oxidative stress and leading to subsequent damage in cells. Our study shows evidence of secondary reactions modifying the primary organic particles emitted in the morning rush hour.

As a wide range of chemical compounds is present both in the particle and gas phase compared to a controlled laboratory experiment, any chemical mechanism is highly speculative. However, by considering different sub-groups within cluster SOA-PAH,

some insights can be gained. Figure 6 shows the difference in positive mass spectra between SOA-PAH particles with high and low peak area at *m/z* 81 ([HSO3]$^-$), an ATOFMS marker for particle acidity. SOA-PAH particle mass spectra with an absolute peak area lower than 2000 are subtracted from those with absolute peak area greater than 10 000. The more acidic the particles (positive values, Fig. 6), the more oxygenated peaks (*m/z* 43, 57, 69 and 81) along with peaks at *m/z* > 100 are seen. On the other hand, when the sulphuric acid content is very low (negative values, Fig. 6) clear organo-nitrogen peaks (likely to be amines) can be seen in less acidic particles (*m/z* 39, 74 and 86 associated with organic-nitrogen species are present), suggesting more acidic particles enhance secondary organic aerosol production.

4.2 Comparison with the AMS findings

In the last decade the AMS instrument has provided invaluable quantitative information upon the aerosol mass loading of generic organic components, including hydrocarbon-like and oxygenated organic aerosols (Canagaratna et al., 2007). Recently, Positive Matrix Factorization (PMF) has been demonstrated to be a powerful tool for the purposes of profiling different components of the ambient organic aerosol data matrix from the Aerodyne Aerosol Mass Spectrometer (AMS). Ulbrich et al. (2009) for example reported three components: hydrocarbon-like organic aerosol (HOA), a highly-oxygenated organic aerosol (OOA) that correlates well with sulfate, and a less-oxygenated, semi-volatile organic aerosol that correlates well with nitrate and chloride. These were identified and interpreted as primary combustion emissions, aged SOA, and semi-volatile, less aged SOA, respectively. Allan et al. (2010) report a detailed analysis of the AMS organic aerosol component sampled during the REPARTEE-I campaign, reporting three components: HOA (25%), OOA (53%) and a factor associated with primary organic aerosols related to cooking emissions COA (22%). A comparison between the ATOFMS and the AMS is not straightforward, as the qualitative temporal information of the ATOFMS particle number concentration of single particle mass spectral type does not allow a meaningful correlation with quantitative aerosol mass loading concentrations of organic components provided by the AMS. A correlation coefficient

(R^2) matrix between ATOFMS particle types (number) and AMS mass concentrations appears in Table 2.

In this study, ATOFMS cluster Ca-EC, as well as cluster OC, correlate highly with the AMS HOA (R^2 = 0.65 and 0.50 respectively), as shown in earlier studies (Drewnick et al., 2008). The AMS factor OOA represents a well-aged secondary organic aerosol, and was found consistent with an atmospheric regionally transported source rather than local meteorology, as reported in Dall'Osto et al. (2009a). It correlates weakly with particle type Na-EC-OC. Beside the commonly measured HOA and OOA factors, a further component, COA exhibited a unique mass spectrum with strong signals at *m/z* 41 and *m/z* 55. However, as noted by Allan et al. (2010), the 3 factor solution approach tended to result in residuals larger than would be considered optimal according to the error model, which indicates that the number of factors used is insufficient to capture all of the chemical variability within the dataset.

The SOA-PAH particle type shows peaks at *m/z* 256 (thought to be hexadecanoic acid) and *m/z* 284 (octadecanoic acid), seen in the negative mass spectrum (Fig. 2). Ning et al. (2007) reported ultrafine particles sampled in the afternoon in Los Angeles to show reduced nitrate concentrations (temperature increasing in the afternoon), to contain more organic matter than the morning samples (more SOA), to be more acidic (less ammonia to neutralize the sulphuric acid), and to be rich in octadecanoic acid and hexadecanoic acids. Whilst Rogge et al. (1993) showed that food cooking is a source of organic acids, it was concluded that atmospheric chemistry is more likely responsible for their formation as food cooking alone cannot explain the atmospheric concentrations measured (Pandis et al., 1993; Rogge et al., 1993). However, far fewer published profiles are available for food cooking relative to motor vehicles and biomass combustion, and significant inconsistencies exist between the ambient data and published source profiles so further studies are required in order to correctly apportion food cooking emissions (Robinson et al., 2006).

Figure 7 shows the average ATOFMS mass spectra of particles containing a peak at *m/z* 55 (peak height > 100), a key peak describing the third AMS factor (COA) solution

(Allan et al., 2010). Figure 7 is an average of about 11 500 particles containing a signal at *m/z* 55 (from here called particle type *m/z* 55). The average mass spectrum shows peaks due to OC (*m/z* 27, *m/z* 41, *m/z* 55, *m/z* 63, *m/z* 77), fragments of large aromatic compounds (*m/z* 115, *m/z* 165), nitrate (*m/z* −46, *m/z* −62) and sulphate (*m/z* −97), all peaks contained within particle types OC, Na-EC-OC and SOA-PAH. The broad similarity of the mass spectra shown in Fig. 7 with particle types OC, Na-EC-OC and SOA-PAH is also reflected in the fact that the total number of particles containing *m/z* 55 broadly follows the sum of the 3 ATOFMS Art-2a clusters (Fig. 4). The temporal trend of particle type *m/z* 55 in Fig. 5e, where a bimodal diurnal profile can be seen peaking at noon and during evening times bears some similarity to the COA factor, but the correlation between the sum of the three ATOFMS types (OC + Na-EC-OC and SOA-PAH) and AMS factor COA is entirely insignificant ($R^2 < 0.1$) (Table 2). It does however raise the question over whether the COA factor is comprised of a number of different particle types arising from different sources. The two instruments involve very different vaporisation/ionisation procedures (ATOFMS by u.v. laser and AMS by heating and electron impact) probably leading to significantly different mass spectral fragmentation patterns in terms of relative peak intensities, if not *m/z* values. The cooking aerosol may be transparent to the u.v. laser, hence failing to ionise in the ATOFMS. The ATOFMS analyses individual particles and therefore sees a particle resulting from coagulation as different from its two parent particles whereas the AMS views an aggregate mass spectrum of particles of all types admitted to the instrument at a specific time. It should also be remembered that the two instruments are responsive to different particle size ranges and that the cooking oil aerosol characterised as the COA factor by the AMS may be of two small a size (<200 nm) to be seen by the ATOFMS. These differences make it very difficult to try to intercompare data from the two instruments, although sometimes data from one can be valuable in informing interpretation of data from the other (e.g. Dall'Osto et al., 2009a; Drewnick et al., 2008). In this dataset, the ATOFMS does not appear to see any particle type characteristic of a cooking source.

5 Conclusions

This work emphasises that neither the AMS nor the ATOFMS alone is able to give a comprehensive insight into aerosol composition and sources. Our earlier work has demonstrated that in combination they give far greater insights into aerosol behaviour than either technique can alone (Dall'Osto et al., 2009a, b) and the work presented here seems to confirm that vision. The AMS has a well proven capability to quantify generic source-related categories of non-refractory aerosol. The ATOFMS gives mass spectral information upon individual particles which, even after clustering particles with similar size distribution and mass spectral characteristics, presents information which can be very difficult to interpret in relation to the sources or atmospheric processing, as is the case with some particle types identified in this study.

The ATOFMS cannot provide quantitative aerosol mass loading concentrations, but its unique strength relies in the fact that it can monitor in real time variations in the single particle composition. Further work is needed in order to attribute mass spectra to particular sources with greater confidence. Comparing laboratory and ambient spectra may not be sufficient to associate a specific mass spectrum to an aerosol source seen in the ambient data, as particles with primary and secondary origins may have broadly similar mass spectra, and particles are modified substantially during atmospheric transport processes. The ATOFMS particle types Ca-EC, which derives from road traffic, and OC, containing organic carbon from primary sources, correlate strongly with the AMS HOA factor. The modest correlation between ATOFMS particle Na-EC-OC and AMS OOA suggests that this is an aged particle type containing mainly secondary organic carbon. ATOFMS type SOA-PAH appears to be a specific component of secondary organic aerosol for which the ATOFMS has high sensitivity, but which does not represent the temporal trends in total secondary aerosol as shown by AMS factor OOA. There is no clear evidence that any ATOFMS particle type, or combination of particle types, corresponds to the AMS COA cooking factor.

Acknowledgements. This research was supported by the UK Natural Environment Research Council as part of the programme of the National Centre for Atmospheric Science. Meteorological data, ozone and NOx data were provided by Eiko Nemitz (CEH Edinburgh). AMS and BC data were provided by Paul Williams, James Allan and Hugh Coe (University of Manchester, UK). James Allan is particularly acknowledged for long helpful discussions on interpretation of AMS data. Alistair Thorpe collected PM data for the REPARTEE-I experiment. The authors are grateful also to the BOC Foundation for financial support of campaign expenses and to British Telecom and the Royal Parks for facilitating access to measurement sites.

References

Allan, J. D., Williams, P. I., Morgan, W. T., Martin, C. L., Flynn, M. J., Lee, J., Nemitz, E., Phillips, G. J., Gallagher, M. W., and Coe, H.: Contributions from transport, solid fuel burning and cooking to primary organic aerosols in two UK cities, Atmos. Chem. Phys., 10, 647–668, doi:10.5194/acp-10-647-2010, 2010.

Bunce, N. J., Liu, L., Zhu, J., and Lane, D. A.: Reaction of naphthalene and its derivatives with hydroxyl radicals in the gas phase, Environ. Sci. Technol., 31, 2252–2259, 1997.

Canagaratna, M. R., Jayne, J. T., Jimenez, J. L., Allan, J. D., Alfarra, M. R., Zhang, Q., Onasc, T. B., Drewnick, F., Coe, H., Middlebrook, A., Delia, A., Williams, L. R., Trimborn, A. M., Northway, M. J., DeCarlo, P. F., Kolb, C. E., Davidovits, P., and Worsnop D. R.: Chemical and microphysical characterization of ambient aerosols with the aerodyne aerosol mass spectrometer, Mass Spectrom. Rev., 26, 185–222, 2007.

Chan, A. W. H., Kautzman, K. E., Chhabra, P. S., Surratt, J. D., Chan, M. N., Crounse, J. D., Kürten, A., Wennberg, P. O., Flagan, R. C., and Seinfeld, J. H.: Secondary organic aerosol formation from photooxidation of naphthalene and alkylnaphthalenes: implications for oxidation of intermediate volatility organic compounds (IVOCs), Atmos. Chem. Phys., 9, 3049–3060, doi:10.5194/acp-9-3049-2009, 2009.

Cuyckens, F. and Claeys, M.: Mass spectrometry in the structural analysis of flavonoids, J. Mass Spectrom., 39, 1–15, 2004.

Dall'Osto, M. and Harrison R. M.: Chemical Characterisation of single airborne particles in Athens (Greece) by ATOFMS, Atmos. Environ., 40, 7614–7631, 2006.

Dall'Osto, M., Harrison, R. M., Beddows, D. C. S., Freney, E. J., Heal, M. R., and Donovan, R. J.: Single-particle detection efficiencies of aerosol time-of-flight mass spectrometry during the North Atlantic marine boundary layer experiment, Environ. Sci.Technol., 40(16), 5029–5035, 2006.

Dall'Osto, M., Harrison, R. M., Coe, H., Williams, P. I., and Allan, J. D.: Real time chemical characterization of local and regional nitrate aerosols, Atmos. Chem. Phys., 9, 3709–3720, doi:10.5194/acp-9-3709-2009, 2009a.

Dall'Osto, M., Harrison, R. M., Coe, H., and Williams, P.: Real-time secondary aerosol formation during a fog event in London, Atmos. Chem. Phys., 9, 2459–2469, doi:10.5194/acp-9-2459-2009, 2009b.

Donahue, N. M., Robinson, A. L., and Pandis, S. N.: Atmospheric organic particulate matter: From smoke to secondary organic aerosol, Atmos. Environ., 43(1), 94–106, 2009.

Drewnick, F., Hings, S. S., DeCarlo, P., Jayne, J. T., Gonin, M., Fuhrer, K., Weimer, S., Jimenez, J. L., Demerjian, K. L., Borrmann, S., and Worsnop D. R.: A new time-of-flight aerosol mass spectrometer (TOF-AMS) – Instrument description and first field deployment, Aerosol Sci. Technol., 39, 637–658, 2005.

Drewnick, F., Dall'Osto, M., and Harrison, R.: Characterization of aerosol particles from grass mowing by joint deployment of ToF-AMS and ATOFMS instruments, Atmos. Environ., 42(13), 3006–3017, 2008.

Gard, E., Mayer, J. E., Morrical, B. D., Dienes, T., Fergenson, D. P., and Prather K. A.: Real-time analysis of individual atmospheric aerosol particles: Design and performance of a portable ATOFMS, Anal. Chem., 69, 4083–4091, 1997.

Goldstein, A. H. and Galbally, I. E.: Known and unexplored organic constituents in the earth's atmosphere, Environ. Sci.Technol., 41, 1514–1521, 2007.

Gross, D. S., Galli, M. E., Silva, P. J., Wood, S. H., Liu, D. Y., and Prather, K. A.: Single particle characterization of automobile and diesel truck emissions in the Caldecott Tunnel, Aerosol Sci. Technol., 32, 152–163, 2000.

Kalberer, M., Paulsen, D., Sax, M., Steinbacher, M., Dommen, J., Prevot, A. S., Fisseha, R., Weingartner, E., Frankevich, V., Zenobi, R., and Baltensperger, U.: Identification of polymers as major components of atmospheric organic aerosols, Science, 303, 1659–1662, 2004.

Kanakidou, M., Seinfeld, J. H., Pandis, S. N., Barnes, I., Dentener, F. J., Facchini, M. C., Van Dingenen, R., Ervens, B., Nenes, A., Nielsen, C. J., Swietlicki, E., Putaud, J. P., Balkanski, Y., Fuzzi, S., Horth, J., Moortgat, G. K., Winterhalter, R., Myhre, C. E. L., Tsigaridis, K., Vignati, E., Stephanou, E. G., and Wilson, J.: Organic aerosol and global climate modelling:

a review, Atmos. Chem. Phys., 5, 1053–1123, doi:10.5194/acp-5-1053-2005, 2005.
Kroll, J. H. and Seinfeld, J. H.: Chemistry of secondary organic aerosol: Formation and evolution of low-volatility organics in the atmosphere, Atmos. Environ., 42, 3593–3624, 2008.
Langford, B., Nemitz, E., House, E., Phillips, G. J., Famulari, D., Davison, B., Hopkins, J. R., Lewis, A. C., and Hewitt, C. N.: Fluxes and concentrations of volatile organic compounds above central London, UK, Atmos. Chem. Phys., 10, 627–645, doi:10.5194/acp-10-627-2010, 2010.
Maul, R., Schebb, N. H., and Kulling, S. E.: Application of LC and GC hyphenated with mass spectrometry as tool for characterization of unknown derivatives of isoflavonoids, Anal. Bioanal. Chem., 391, 239–250, 2008.
McLafferty, F. W.: Interpretation of Mass Spectra, third ed., 303 pp., 1983.
Mihele, C. M., Wiebe, H. A., and Lane, D. A.: Particle formation and gas/particle partition measurements of the products of the naphthalene-OH radical reaction in a smog chamber, Polycycl. Aromat. Comp., 22, 729–736, 2002.
Murphy, D. M.: The design of single particle laser mass spectrometers, Mass Spectrom. Rev., 26, 150–165, 2007.
Ning, Z., Geller, M. D., Moore, K. F., Sheesley, R., Schauer, J. J., and Sioutas, C.: Daily variation in chemical characteristics of urban ultrafine aerosols and inference of their sources, Environ. Sci.Technol., 41, 6000–6006, 2007.
Pandis, S. N., Wexler, A. S., and Seinfeld, J. H.: Secondary organic aerosol formation and transport.2. Predicting the ambient secondary organic aerosol-size distribution, Atmos. Environ., Part A-General Topics, 27, 2403–2416, 1993.
Petzold, A. and Schonlinner, M.: Multi-angle absorption photometry - a new method for the measurement of aerosol light absorption and atmospheric black carbon, J. Aerosol Sci., 35, 421–441, 2004.
Qin, X. Y., Bhave, P. V., and Prather, K. A.: Comparison of two methods for obtaining quantitative mass concentrations from aerosol time-of-flight mass spectrometry measurements, Anal. Chem., 78(17), 6169–6178, 2006.
Reinard, M. S. and Johnston, M. V.: Ion formation mechanism in laser desorption ionization of individual nanoparticles, J. Am. Soc. Mass Spectrom., 19, 389–399, 2008.
Robinson, A. L., Subramanian, R., Donahue, N. M., Bernardo-Bricker, A., and Rogge, W. F.: Source apportionment of molecular markers and organic aerosol, 3. Food cooking emissions, Environ. Sci. Technol., 40, 7820–7827, doi:10.1021/Es060781p, 2006.

Robinson, A. L., Donahue, N. M., Shrivastava, M. K., Weitkamp, E. A., Sage, A. M., Grieshop, A. P., Lane, T. E., Pierce, J. R., and Pandis, S. N.: Rethinking organic aerosols: Semivolatile emissions and photochemical aging, Science, 315, 1259–1262, 2007.
Rogge, W. F., Hildemann, L. M., Mazurek, M. A., Cass, G. R., and Simoneit, B. R. T.: Sources of fine organic aerosol.2. Noncatalyst and catalyst-equipped automobiles and heavy-duty diesel trucks, Environ. Sci.Technol., 27, 636–651, 1993.
Sasaki, J., Aschmann, S. M., Kwok, E. S. C., Atkinson, R., and Arey, J.: Products of the gas-phase OH and NO3 radical-initiated reactions of naphthalene, Environ Sci Technol., 31, 3173–3179, 1997.
Schauer, J. J., Kleeman, M. J., Cass, G. R., and Simoneit, B. R. T.: Measurement of emissions from air pollution sources. 2. C- 1 through C-30 organic compounds from medium duty diesel trucks, Environ. Sci. Technol., 33, 1578–1587, 1999.
Schauer, J. J., Kleeman, M. J., Cass, G. R., and Simoneit, B. R. T.: Measurement of emissions from air pollution sources. 3. C-1-C- 29 organic compounds from fireplace combustion of wood, Environ. Sci. Technol., 35, 1716–1728, 2001.
Silva, P. J. and Prather K. A.: Interpretation of mass spectra from organic compounds in aerosol time-of-flight mass spectrometry, Anal. Chem., 72, 3553–3562, 2000.
Silva, P. J., Liu, D.-Y., Noble, C. A., and Prather, K. A.: Size and chemical characterization of individual particles resulting from biomass burning of local Southern California species, Environ. Sci. Technol., 33(18), 3068–3076, 1999.
Song, X. H., Hopke, P. K., Fergenson, D. P., and Prather, K. A.: Classification of single particles analyzed by ATOFMS using an artificial neural network, ART-2A, Anal. Chem., 71(4), 860–865, 1999.
Spencer, M. T., Shields, L. G., Sodeman, D. A., Toner, S. M., and Prather, K. A.: Comparison of oil and fuel particle chemical signatures with particle emissions from heavy and light duty vehicles, Atmos. Environ., 40, 5224–5235, 2006.
Sullivan, R. C. and Prather, K. A. Recent advances in our understanding of atmospheric chemistry and climate made possible by on-line aerosol analysis instrumentation, Anal. Chem., 77(12), 3861–3885, 2005.
Toner, S.: Source characterization and source apportionment of anthropogenic aerosols, PhD Thesis, UCSD, California, USA, 2008.
Ulbrich, I. M., Canagaratna, M. R., Zhang, Q., Worsnop, D. R., and Jimenez, J. L.: Interpretation of organic components from Positive Matrix Factorization of aerosol mass spectrometric

data, Atmos. Chem. Phys., 9, 2891–2918, doi:10.5194/acp-9-2891-2009, 2009.
Verma, V., Ning, Z., Cho, A. K., Schauer, J. J., Shafer, M. M., and Sioutas C.: Redox activity of urban quasi-ultrafine particles from primary and secondary sources, Atmos. Environ., 43, 6360–6368, 2009.
Walgraeve, C., Demeestere, K., Dewulf, J., Zimmermann, R., and Van Langenhove, H.: Oxygenated polycyclic aromatic hydrocarbons in atmospheric particulate matter: Molecular characterization and occurrence, Atmos. Environ., 44, 1831–1846, 2010.
Wang, L., Atkinson, R., and Arey, J.: Dicarbonyl products of the OH radical-initiated reactions of naphthalene and the C-1- and C-2-alkylnaphthalenes, Environ. Sci. Technol., 41, 2803–2810, 2007.
Webb, P. J., Hamilton, J. F., Lewis, A. C., and Wirtz, K.: Formation of oxygenated-polycyclic aromatic compounds in aerosol from the photo-oxidation of o-tolualdehyde, Polycyclic Aromatic Compounds, 26, 237–252, 2006.
Whiteaker, J. R. and Prather, K. A.: Hydroxymethanesulfonate as a tracer for fog processing of individual aerosol particles, Atmos. Environ., 37, 1033–1043, 2003.

Table 1. ATOFMS particle clusters identified from the REPARTEE campaign.

Main	ATOFMS cluster	N particles	% cluster
Secondary OA	LRT nitrate	43 516	33.7
	LRT core	10 278	8.0
	Local nitrate	29 563	22.9
	Amine	2306	1.8
	HMOC (fog)	4865	3.8
	MSA (fog)	245	0.2
	SOA-PAH	2834	2.2
Primary OA	Ca-EC	5496	4.3
	OC	4671	3.6
	PAH	269	0.2
	EC	2001	1.5
	Na-OC-EC	2207	1.7
Inorganic	NaCl only	3637	2.8
	Aged NaCl	15 638	12.1
	Fe	1748	1.4
	TOTAL	**129 274**	**100.0**

Table 2. Correlations (R^2) between ATOFMS organic particle types (number) and AMS concentrations averaged over 3-h intervals.

3 h resolution	AMS OOA	AMS HOA	AMS COA	AMS org
ATOFMS Ca-EC	< 0.1	0.65	< 0.1	0.12
ATOFMS OC	< 0.1	0.50	< 0.1	0.14
ATOFMS Na-EC-OC	0.35	−0.1	< 0.1	0.14
ATOFMS SOA-PAH	< 0.1	< 0.1	0.15	< 0.1

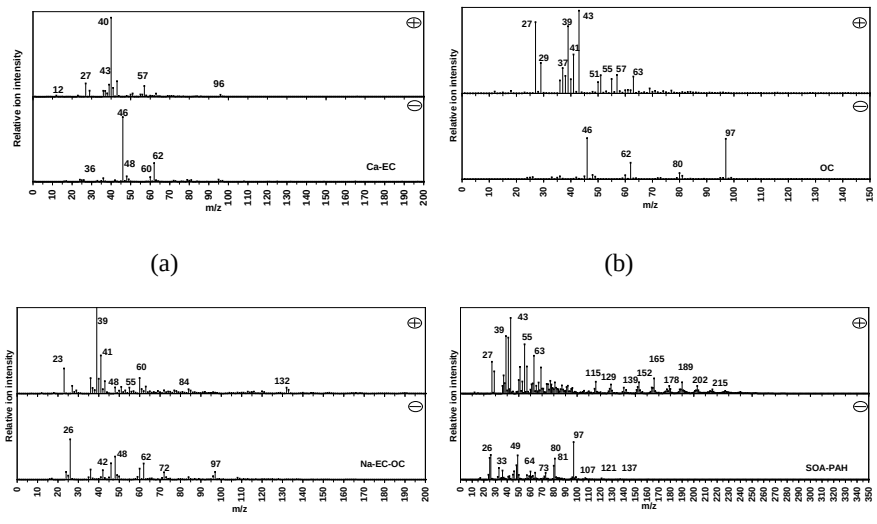

Fig. 1. Positive and Negative ART-2a area vectors attributed to **(a)** Ca-EC, **(b)** OC, **(c)** Na-EC-OC and **(d)** SOA-PAH.

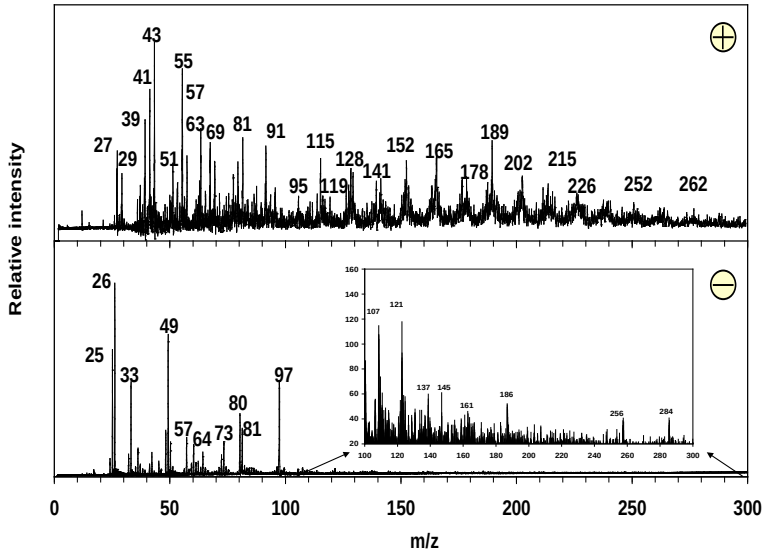

Fig. 2. Single particle positive and negative mass spectra of an individual particle belonging to ART-2a cluster SOA-PAH.

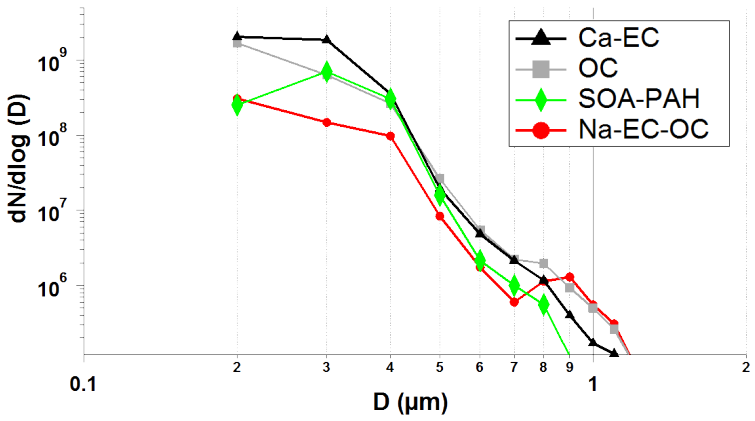

Fig. 3. Size distributions of the 4 ATOFMS particle types described in Fig. 1.

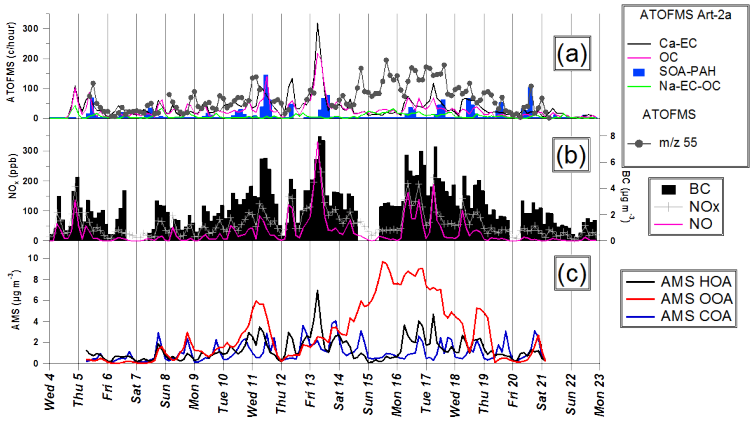

Fig. 4. Temporal trends of **(a)** ATOFMS clusters described in Fig. 1, **(b)** BC and nitrogen gases and **(c)** AMS profiles as reported in Allan et al. (2010).

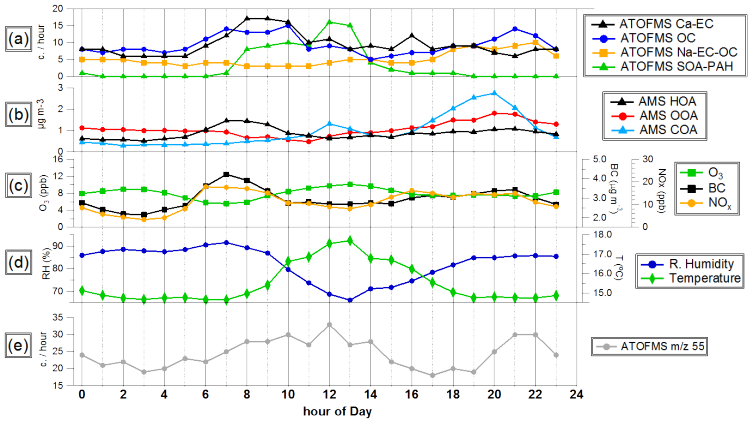

Fig. 5. Average diurnal profiles for **(a)** ATOFMS cluster described in Fig. 1, **(b)** AMS PMF factors as reported in Allan et al. (2010); **(c)** ozone, NO_x and black carbon concentrations; **(d)** relative humidity and temperature and **(e)** ATOFMS hit particles with *m/z* 55 (peak height > 100).

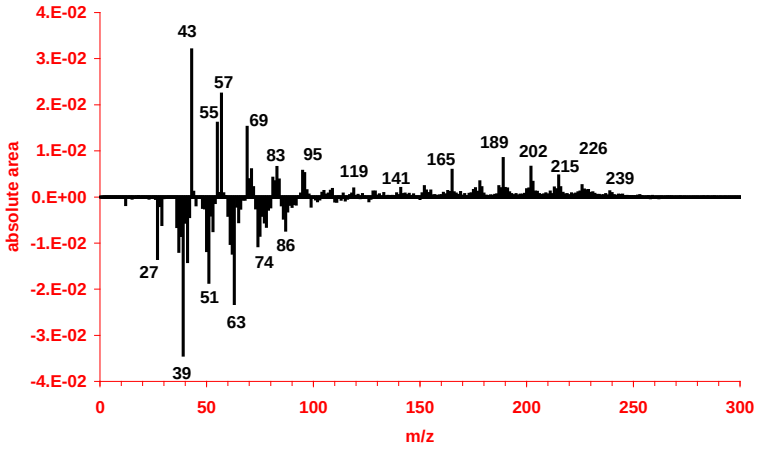

Fig. 6. Positive and negativeART-2a area vectors differences for the positive mass spectra (cluster SOA-PAH with high content HSO_3^- and little content; peak area *m/z* −81 > 10 000 and *m/z* −81 < 2000 respectively).

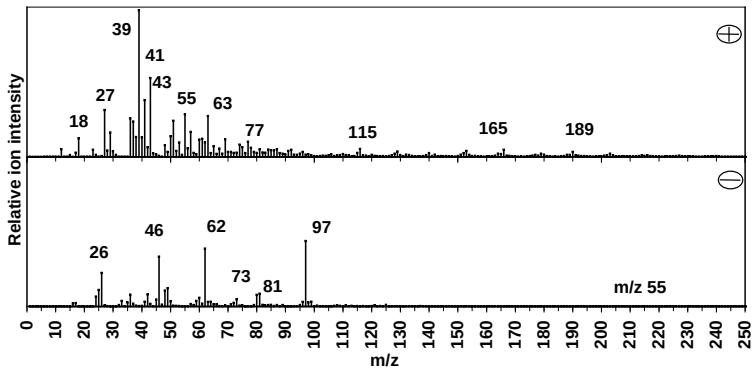

Fig. 7. Average mass spectra for all hit particles during the REPARTEE I campaign containing values of peak height at *m/z* 55 higher than 100.